Edited by S. Selberherr, H. Stippel, E. Strasser – September 1993

Numerical Modeling of Electrothermal Effects in Semiconductor Devices

Y. Apanovich, B. Cottle, B. Freydin, E. Lyumkis, B. Polsky, and P. Blakey

Algorithms Development Group, Silvaco International
4701 Patrick Henry Drive, Bldg. 3, Santa Clara, CA 95054, USA

Abstract

Nonisothermal steady-state and transient simulation capabilities have been implemented in the ATLAS general purpose 2D device simulator. The new capabilities support accurate simulation of silicon and heterostructure devices, taking into account lattice heating, heat sinks and other features of the thermal environment. Results of self-consistent simulations of HBT, HEMT and ESD protection devices are presented and compared with results obtained using isothermal simulation.

1. Introduction

Numerical simulation of electrothermal processes is important for the design and optimization of many semiconductor devices, including power devices, electrostatic discharge (ESD) protection devices, SOI MOSFET's, and heterojunction devices. General electrothermal simulation capabilities have now been incorporated into the ATLAS [1] general purpose 2D device simulator. The ability of ATLAS to simulate electrothermal effects is illustrated by results obtained for steady-state simulation of AlGaAs/GaAs HBT and HEMT devices, and for transient simulation of a silicon ESD protection device.

2. Physical Model and Numerical Techniques

The electrothermal capabilities in ATLAS are based on Wachutka's thermodynamically rigorous model [2]. The current density equation includes terms that deal with variable band structure and thermal diffusion [3, 4]. The main heat source in the lattice heat equation is Joule heat. Generation/recombination heat, and Thomson and Peltier terms are also included in Wachutka's model. These terms can be switched off in the ATLAS implementation to recover the 'intuitive' ($J_n \cdot \nabla E_c + J_p \cdot \nabla E_v$) model. The dependencies of all physical parameters on lattice temperature are modeled. These dependecies lead to reduced mobilities and ionization coefficients with increasing temperature for a given electric field.

Very general thermal environments can be simulated. Realistic multi-layer heat sink structures may be specified. Thermal boundary conditions may be specified in terms of temperature, heat flux, or thermal impedance. The latter capability is useful for handling certain situations (e.g. thick substrates) in a computationally efficient manner.

The discrete nonlinear problem is solved using an iterative scheme in which Newton iteration or Gummel's method is used to solve Poisson's equation and the current continuity equations, and then the heat flow equation is solved. This approach is used for both steady-state and transient calculations.

3. Results

3.1. AlGaAs/GaAs HBT Example

Calculations that include electrothermal effects in a AlGaAs/GaAs HBT were simulated and compared to isothermal results calculated at T=300 K. Thermoisolation was assumed at all boundaries except for the substrate boundary which was modeled using a thermal resistor. Values for the thermal resistor of 0.0005 cm^2 K/W and 0.002 cm^2 K/W were considered. Figure 1 shows calculated common emitter I-V characteristics with Ib=0.5μA/μm and Ib=2μA/μm. The non-isothermal simulations predict lower currents than the isothermal calculations. The decrease is believed to be due to decreased mobility as the temperature increases. The temperature distribution in the device is shown in Figure 2 for Ib=2μA/μm, Vcol=4V, and Rth=0.002 cm^2 K/W. The temperature varies smoothly in the device with a peak value in the vicinity of the collector-base junction.

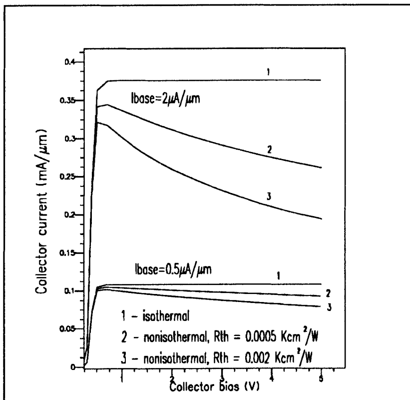

Figure 1. Common emitter I-V characteristics for the AlGaAs/GaAs HBT.

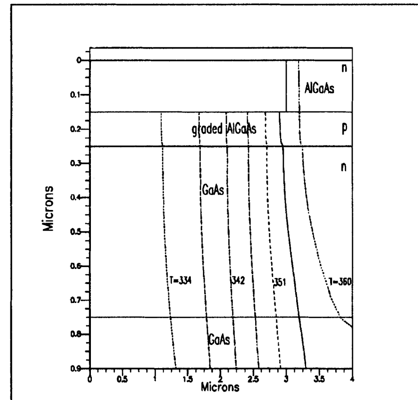

Figure 2. Temperature distribution in the HBT. Ib=2μA/μm, Vcol=4V, Rth=0.002cm^2 K/W.

3.2. AlGaAs/GaAs HEMT Example

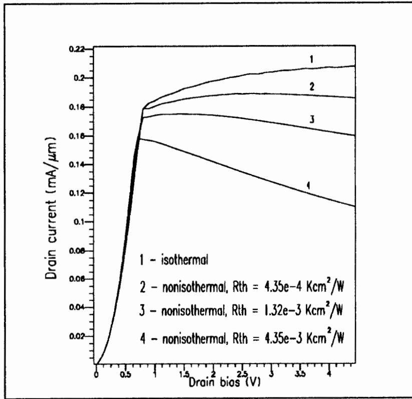

Figure 3. Id-Vd curves for the AlGaAs/GaAs HEMT.

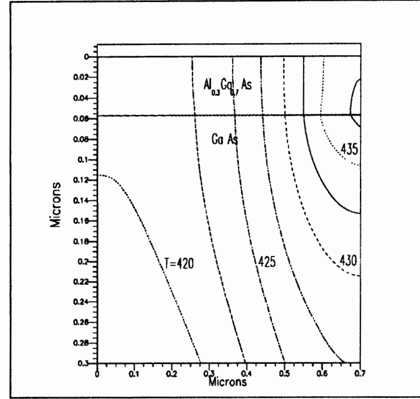

Figure 4. Temperature distribution in the HEMT for Vd=4V, Vg=0, Rth = 0.00132 cm^2 K/W.

A similar reduction of drain current in nonisothermal calculations, as compared with isothermal calculations, takes place in HEMT's. Figure 3 shows the calculated drain currents versus drain voltage for Vg=0. Three values of thermal resistance were used to model the effect of different heat sinks. As can be seen from Figure 3, a thermally-induced negative differential resistance may arise. The calculation with Rth=0.00435 cm^2 K/W models an extreme case with a poor heat sink. The calculated temperature distribution in the HEMT for V_d=4V, Rth=0.00132 cm^2 K/W is shown in Figure 4.

3.3. Transient Simulation of Si ESD Protection Device

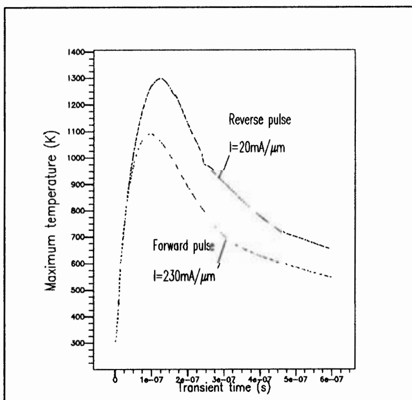

Figure 5. Maximum temperature in ESD protection device as function of time.

Electrothermal transients in a silicon ESD protection device were simulated under conditions of stress induced by an ESD human body model pulse. The current pulse was applied to the n-contact. A linear ramp of 10ns duration and a peak amplitude of 230 mA/μm for the forward pulse and 20 mA/μm for the reverse pulse was followed by exponential current decrease with a characteristic decay time of 150ns. The maximum temperature in the structure versus time is shown in Figure 5.

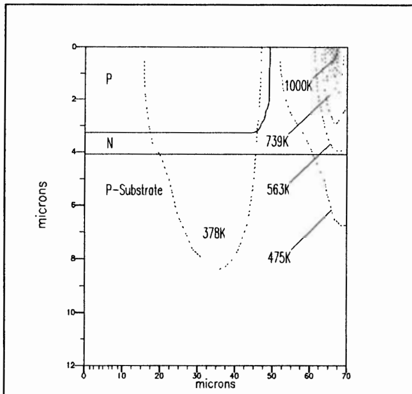

Figure 6. Temperature distribution in ESD protection device. Forward current pulse, t=92 ns.

A temperature distribution for the case of a forward current pulse at t=92 ns is shown in Figure 6. The location of a "hot spot" is clearly visible.

Knowledge of the internal temperature distributions helps device designers to identify failure mechanisms, and evaluate alternative designs.

4. Summary

A self-consistent electrothermal model of lattice heating has been incorporated into a general purpose 2D device simulator. Steady-state and transient capabilities are included, and heat sinks and general thermal boundary conditions are supported. Calculated results demonstrate the influence of thermal effects on the operating characteristics of HBT, HEMT, and ESD protection devices.

References

[1] *ATLAS II Version 1.0 User Manual,* SILVACO International, Santa Clara, 1993.

[2] G. K. Wachutka, "*Rigorous Thermodynamic Treatment of Heat Generation and Conduction in Semiconductor Device Modelling,*" IEEE Trans., CAD-9, pp. 1141-1149, 1990.

[3] J. E. Sutherland and J. R. Hauser, "*A Computer Analysis of Heterojunction and Graded Composition Solar Cells,*" IEEE Trans., ED-24, pp. 363-372, 1977.

[4] A. H. Marshak and K. M. van Vliet, "*Electrical Current in Solids with Position-Dependent Band Structure,*" Solid State Electron., vol. 21, pp. 417- 427, 1978.